

## Supporting Information

### Topological dissection of the membrane transport protein Mhp1 derived from cysteine accessibility and mass spectrometry

Antonio N. Calabrese<sup>1,2</sup>, Scott M. Jackson<sup>1,3,§</sup>, Lynsey N. Jones<sup>1,2</sup>, Oliver Beckstein<sup>4</sup>, Florian Heinke<sup>5</sup>, Joerg Gsponer<sup>5</sup>, David Sharples<sup>1,3</sup>, Marta Sans<sup>6</sup>, Maria Kokkinidou<sup>6</sup>, Arwen R. Pearson<sup>6</sup>, Sheena E. Radford<sup>1,2</sup>, Alison E. Ashcroft<sup>\*1,2</sup>, Peter J.F. Henderson<sup>\*1,3</sup>

<sup>1</sup> Astbury Centre for Structural Molecular Biology, <sup>2</sup> School of Molecular and Cellular Biology and <sup>3</sup> School of Biomedical Sciences, University of Leeds, Leeds, LS2 9JT, UK.

<sup>4</sup> Department of Physics, Arizona State University, Tempe, AZ, 85287-1504, USA

<sup>5</sup> Centre for High-Throughput Biology, University of British Columbia, Vancouver, BC V6T 1Z4, Canada

<sup>6</sup> Hamburg Centre for Ultrafast Imaging, Institute for Nanostructure and Solid State Physics, Universität Hamburg, Hamburg 22761, Germany

§ Current address: Department of Biology, Institute of Molecular Biology and Biophysics, ETH Zurich, 8093 Zurich, Switzerland

\*Corresponding authors: p.j.f.henderson@leeds.ac.uk, a.e.ashcroft@leeds.ac.uk,

### Table of Contents

#### **Supplementary Methods**

Measurement of the intact mass of Mhp1

Proteolysis and localization of the reaction sites for NEM in individual peptides

Mhp1 ligand binding assays

#### **Supplementary Figures**

Figure S1. Mass spectrometry of wild-type Mhp1, and wild-type Mhp1 labelled with NEM.

Figure S2. Sequencing and residue-specific localisation of modification sites in Mhp1.

Figure S3. Mass spectrometry of wild-type Mhp1 after labeling with NEM under different conditions of substrate and/or Na<sup>+</sup> inclusion.

Figure S4. Titrations of Mhp1 with L-BH and NaCl monitored by NEM labelling.

Figure S5. Equilibrium between inward-facing and outward-facing forms determined by mass spectrometry.

Figure S6. Equilibria for binding and dissociation of cation and ligand determined by spectrophotofluorimetry.

Figure S7. Substitutions of selected amino acid in the ligand binding site affects the labeling of Mhp1 by NEM.

#### **Supplementary Table**

**Table S1.** Theoretical and observed masses of Mhp1, Mhp1 variants and modified proteins

## Supplementary Methods

### *Measurement of the intact mass of Mhp1*

The sample (2  $\mu\text{L}$ ) was loaded onto a MassPREP protein desalting column (Waters Ltd., Manchester), that was washed with 2% (v/v) solvent B in solvent A (solvent A was 0.1% (v/v) formic acid in water, solvent B was 0.1% (v/v) formic acid in acetonitrile) for 5 min at 40  $\mu\text{L min}^{-1}$ . After valve switching, the bound proteins were eluted using a fast gradient of 2-40% solvent B in A over 1 min at 0.5  $\mu\text{L min}^{-1}$ . The column was subsequently washed with 95 % solvent B in A for 6 min and re-equilibrated with 5% B in A for the next injection. The column eluant was infused into a Xevo G2-S mass spectrometer (Waters Ltd, Wilmslow, Manchester, UK). Data processing was performed using MassLynx v 4.1 (Waters Ltd, Wilmslow, Manchester, UK) and deconvolution was performed using UniDec.<sup>1</sup> All expected and observed protein masses are shown in Table S1.

### *Proteolysis and localization of the reaction sites for NEM in individual peptides*

Peptides (1  $\mu\text{L}$ ) were injected onto an Acquity M-Class C18, 75  $\mu\text{m}$  x 150 mm column (Waters Ltd., Wilmslow, Manchester, UK) and separated by gradient elution of 1-50% solvent B (0.1% (v/v) formic acid in acetonitrile) in solvent A (0.1% (v/v) formic acid in water) over 60 min at 300  $\text{nL}\cdot\text{min}^{-1}$ .

The Synapt G2-Si HDMS (Waters Ltd., Wilmslow, Manchester, UK) was operated in positive TOF mode with a capillary voltage of 3.0 kV, a cone voltage of 20 V, a trap bias of 4 V, and a source temperature of 80 °C. Argon was used as the buffer gas in the trap and transfer regions at a pressure of  $8.5 \times 10^{-3}$  mBar. Mass calibration was performed by infusion of aqueous sodium iodide at a concentration of 2  $\mu\text{g}/\mu\text{l}$ . [Glu<sup>1</sup>]-Fibrinopeptide B (GluFib) was used as a lock mass calibrant with a 0.5 second lock spray scan taken every 30 seconds during acquisition. The lock mass correction factor was determined by averaging ten scans. Data acquisition was performed in DDA mode with a one second MS scan over an  $m/z$  range of 350-2000. The four most intense ions in the MS spectrum were selected for MS/MS, each with a 0.5 second scan over an  $m/z$  range of 50-2000. The collision energy applied was dependent upon the charge and mass of the selected ion. Dynamic exclusion of 60 seconds was used. Data processing and modification localization was performed using PEAKS Studio 7 (Bioinformatics Solutions, Ontario, Canada).

### *Mhp1 ligand binding assays*

A sample of Mhp1 (200  $\mu\text{g}/\text{mL}$ ) solubilized in 10 mM Tris.HCl (pH 8), 2.5 % (v/v) glycerol, 0.05% (w/v) DDM, was equilibrated to 20 °C in the spectrofluorometer. Tryptophan fluorescence of protein samples was excited at 295 nm and the intrinsic fluorescence emission at 330 nm was monitored. Micromolar additions of ligand (L-BH) were performed from 0-2 mM. Samples were mixed for 1 min after each addition before the fluorescence emission spectrum was measured. Non-linear regression analysis was performed by fitting to a Michaelis-Menten model using GraphPad Prism 7 (GraphPad Software, San Diego, CA, USA).

## Supplementary Figures

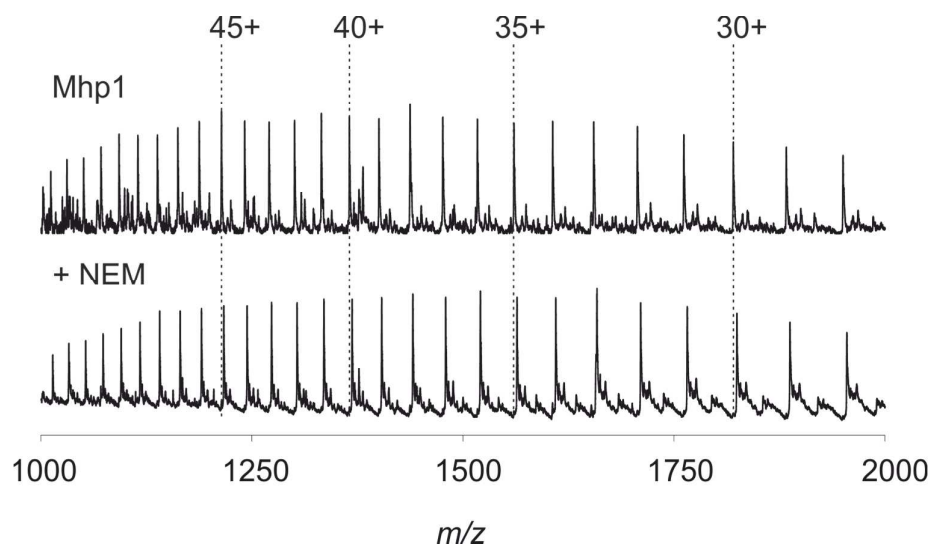


**Figure S1. Mass spectrometry of wild-type Mhp1, and wild-type Mhp1 labelled with NEM.** Representative unprocessed mass spectra of Mhp1 (upper panel) and NEM labelled Mhp1 that was preincubated with 15-crown-5 to remove residual NaCl (lower panel). Spectra were obtained by online desalting-MS. Deconvoluted spectra are shown in Figure 2c.

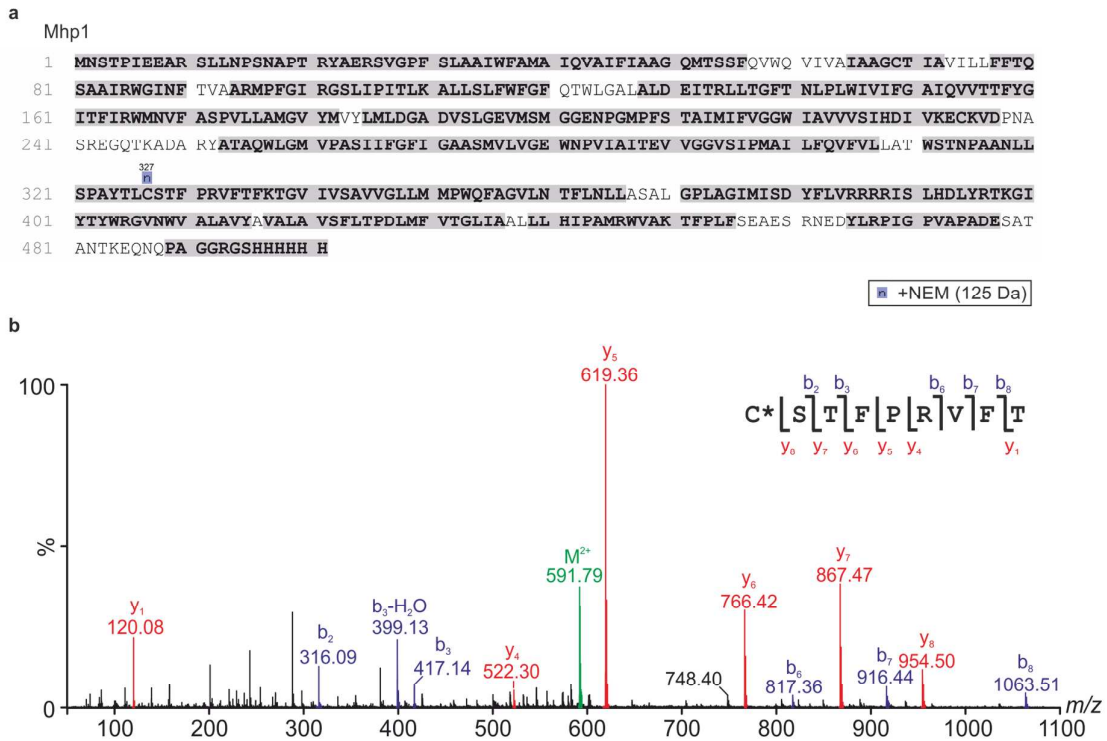


**Figure S2. Sequencing and residue-specific localisation of modification sites in Mhp1.** (a) Typical peptide coverage map, showing the regions of Mhp1 identified by sequencing of peptic peptides in grey. Confidently identified modification sites with > 1 % total ion intensity are shown on the map. The only identified site under these analysis conditions is at Cys327. Typically, the sequence coverage obtained was ca. 87 %. (b) Typical MS/MS spectrum of a peptide from Mhp1 containing NEM-labelled Cys327. The precursor ion is coloured green and the identified b and y ions are coloured in blue and red, respectively.

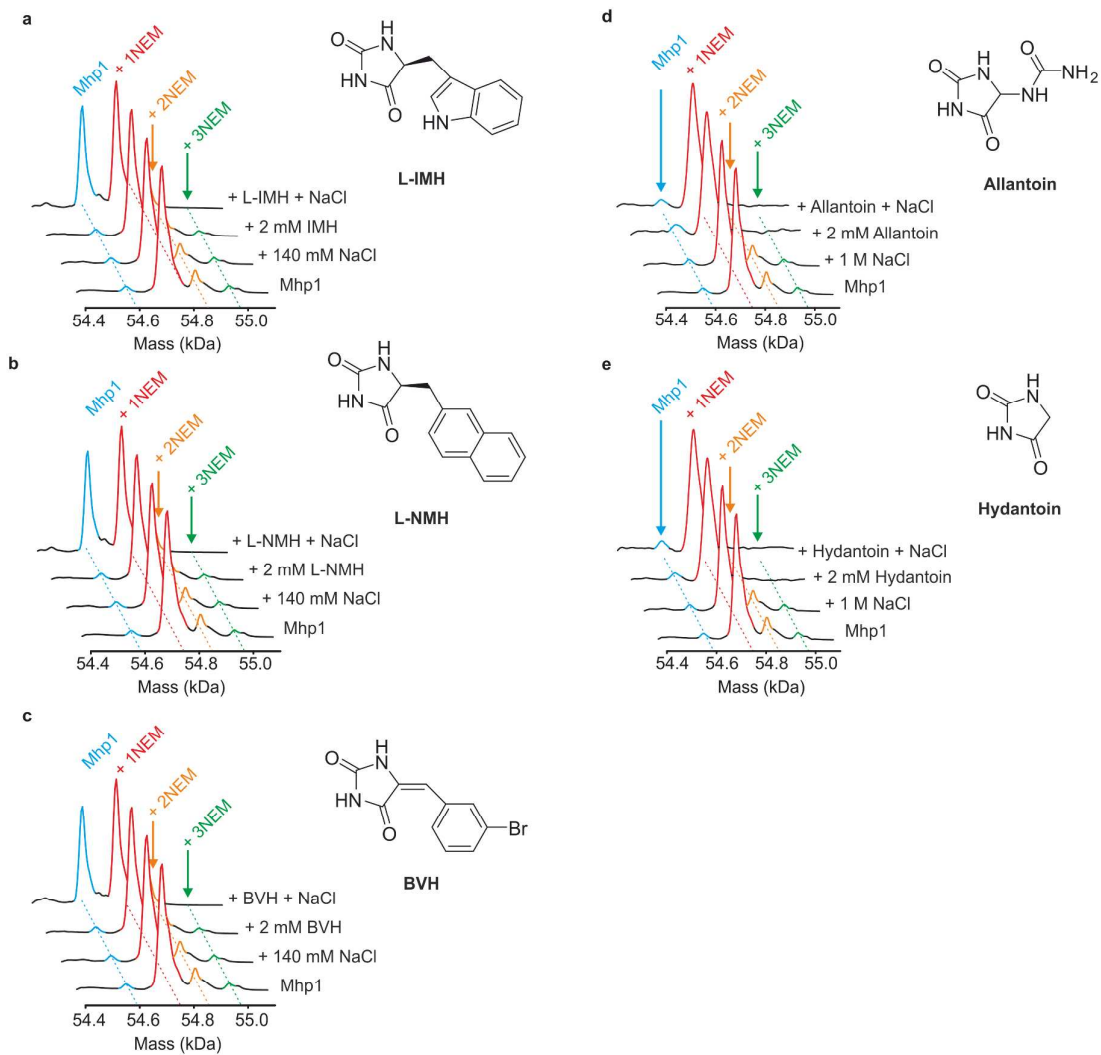


**Figure S3. Mass spectrometry of wild-type Mhp1 after labeling with NEM under different conditions of substrate and/or  $\text{Na}^+$  inclusion.** Deconvoluted mass distributions of Mhp1 after NEM labelling under varied solution conditions (in the presence of 1.25 mM 15-crown-5 (front), 140 mM NaCl (second), 2 mM ligand (third), 2 mM ligand and 140 mM NaCl (back)). Ligands added were **(a)** L-IMH, **(b)** L-NMH, **(c)** BVH, **(d)** allantoin and, **(e)** hydantoin.

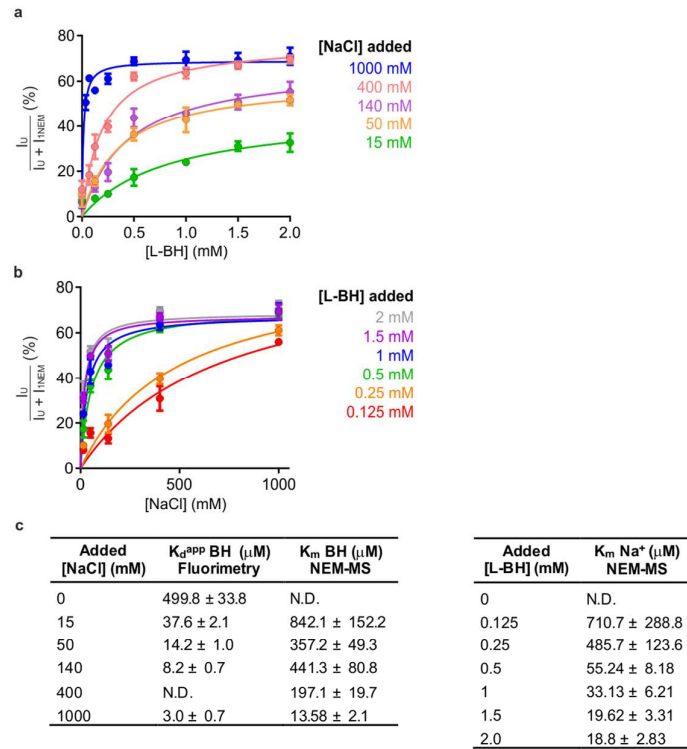


**Figure S4. Titrations of Mhp1 with L-BH and NaCl monitored by NEM labelling. (a)** Quantification of unlabelled Mhp1 as a function of increasing [L-BH], at various concentrations of NaCl. **(b)** Quantification of unlabelled Mhp1 as a function of increasing [NaCl], at various concentrations of L-BH. Data are shown as mean  $\pm$  SEM of three independent measurements. **(c)**  $K_d^{app}$  values for all fluorescence and  $K_m$  values for all NEM-MS titrations. N.D. = not determined.

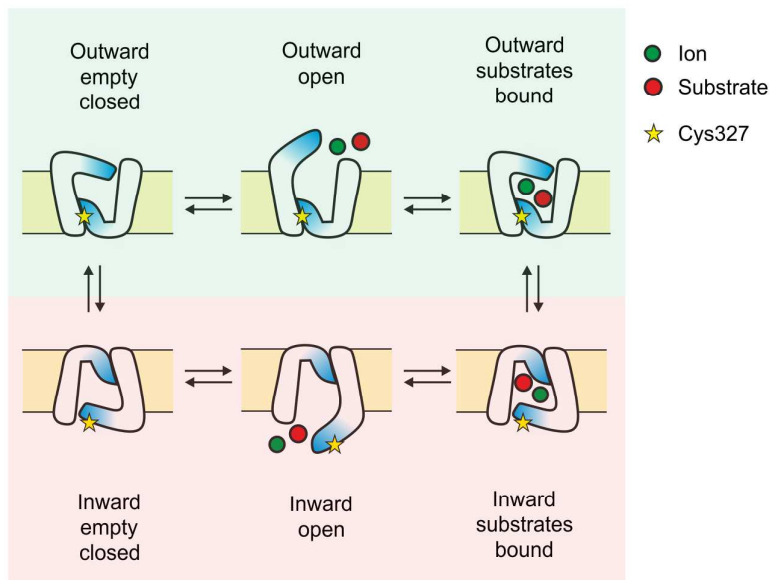


**Figure S5. A typical representation of the alternating access mechanism of secondary active membrane transport<sup>2-3</sup> (Adapted with permission from Ref. <sup>2</sup> Elsevier, 2010). The equilibrium between inward-facing and outward-facing forms is determined by mass spectrometry.** Starting at the top left (and then moving clockwise), the protein is facing outwards but is closed. The protein opens to the outside admitting the two substrates (ion green, ligand red, top middle) and closes to the outside (top right). The protein then undergoes a conformational change to an inward-facing closed conformation (bottom right), before opening to release the substrates on the inside (bottom middle), and then closing to give the apo inward-facing form (bottom left). Thereafter, a conformational change occurs that restores the outward-facing closed form (top left) and the cycle is repeated. The red shading highlights all the inward-facing forms of Mhp1 where Cys327 would react with NEM, while the green shading highlights all the outward-facing forms that, in Mhp1, would not react with NEM. Quantification of the amounts of all the outward-facing forms relative to all the inward-facing forms by NEM-MS (as a function of ion/substrate concentrations) yields a  $K_m$  value reflecting the distribution of all forms of the protein between inward/outward-facing.

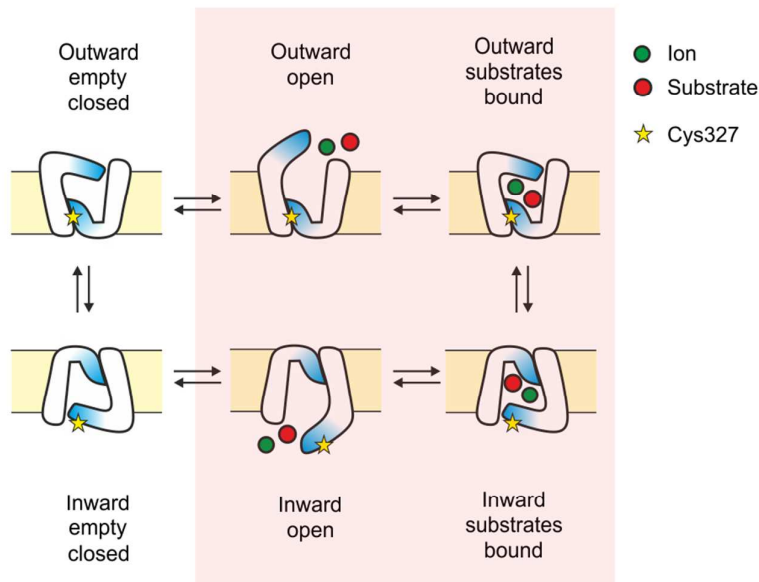


**Figure S6. A typical representation of the alternating access mechanism of secondary active membrane transport<sup>2-3</sup> (Adapted with permission from Ref.<sup>2</sup> Elsevier, 2010). The equilibria for binding and dissociation of cation and ligand are determined by spectrophotofluorimetry.** The same scheme of alternating access is shown as in Figure S5. Spectrophotofluorimetry detects the binding of the ligand to both inward- and outward-facing forms, yielding an apparent  $K_d$  that represents the equilibria between all the forms indicated by the shading in red. This apparent  $K_d$  responds systematically to increasing concentrations of  $\text{Na}^+$  and BH, but they are not expected to be the same as those determined by NEM-MS, because the forms of the protein involved are different (Figure S5).



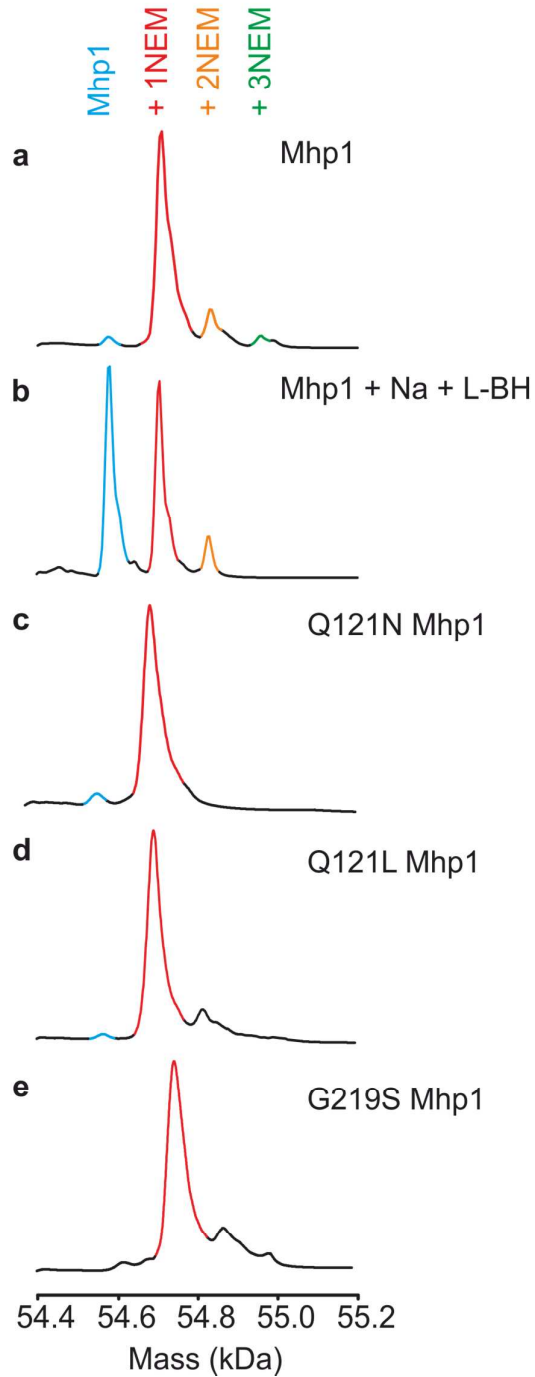


**Figure S7. Substitutions of selected amino acid in the ligand binding site affects the labeling of Mhp1 by NEM.** Deconvoluted mass distributions of (a) WT Mhp1 in the presence of 1.25 mM 15-crown-5, (b) WT Mhp1, (c) Q121N Mhp1, (d) Q121L Mhp1, (e) G219S Mhp1, all in the presence of 140 mM NaCl and 2 mM L-BH.

**Table S1.** Theoretical and observed masses of Mhp1, Mhp1 variants and modified proteins (n.o. = not observed).

Protein	Theoretical Mass (Da)	Observed Mass (Da)
Mhp1	54581.2	54581.9
+ NEM	54706.3	54709.4
+ 2 NEM	54831.5	54831.8
+ 3 NEM	54956.6	54953.7
Q42F Mhp1	54600.3	54601.8
+ NEM	54725.4	54727.1
+ 2 NEM	54850.6	54849.5
+ 3 NEM	54975.7	54974.5
N318A Mhp1	54538.18	54541.6
+ NEM	54663.3	54671.0
+ 2 NEM	54788.4	54790.6
+ 3 NEM	54913.6	54917.8
Q121N Mhp1	54567.2	54570.6
+ NEM	54692.3	54699.2
+ 2 NEM	54942.6	n.o.
+ 3 NEM	55318.0	n.o.
Q121L Mhp1	54566.3	54566.5
+ NEM	54691.4	54694.9
+ 2 NEM	54941.7	n.o.
+ 3 NEM	55317.1	n.o.
G219S Mhp1	54611.2	54614.7
+ NEM	54736.4	54743.7
+ 2 NEM	54986.6	n.o.
+ 3 NEM	55362.0	n.o.

### Supplementary References

- (1) M. T. Marty, A. J. Baldwin, E. G. Marklund, G. K. Hochberg, J. L. Benesch, C. V. Robinson, *Anal Chem* 2015, *87*. 4370-6.
- (2) O. Boudker, G. Verdon, *Trends Pharmacol Sci* 2010, *31*. 418-426.
- (3) P. J. F. Henderson, *Comprehensive Biophysics, Vol 8: Bioenergetics* 2011. 265-288.